OPEN ACCESS

University of BRISTOL

Zhang, W., Zhou, Z., Scarpa, F., & Zhao, S. (2016). A fatigue damage meso-model for fiber-reinforced composites with stress ratio effect. Materials and Design, 107, 212-220. DOI: 10.1016/j.matdes.2016.06.040

Peer reviewed version

License (if available):
CC BY-NC-ND

Link to published version (if available):
10.1016/j.matdes.2016.06.040

Link to publication record in Explore Bristol Research
PDF-document

University of Bristol - Explore Bristol Research

General rights

A fatigue damage meso-model for fiber-reinforced composites with stress ratio effect

Wenjiao Zhang[a,b,c*], Zhengong Zhou[b], Fabrizio Scarpa[c], Shuyuan Zhao[b*]

[a] School of Engineering, Northeast Agricultural University, Harbin, 150030, China

[b] Center for Composite Materials and Structures, Harbin Institute of Technology, Harbin, 150080, China

[c] Advanced Composites Center for Innovation and Science, University of Bristol, Bristol BS8 1TR, UK

Abstract

This work presents a fatigue damage meso-model for fiber-reinforced plastic composites, in which the effect of stress ratios on the off-axis fatigue behavior is taken into account. The non-dimensional effective stress concept is introduced in the continuum damage mechanics method. Damage growths and fatigue failure are studied along axial, transverse and shear directions at meso-scale level. The proposed model is validated through numerical simulations that describe the meso fatigue damage accumulation and the fatigue life for off-axis unidirectional fiber-reinforced plastic composite laminates of arbitrary fiber orientation under different stress ratios. It is shown that the fatigue damage behavior and fatigue life for off-axis unidirectional glass/epoxy and carbon/epoxy composite laminates are adequately described by the proposed fatigue model over the range of different stress ratios.

Keywords: fiber-reinforced composite, fatigue damage, meso-model, continuum damage mechanics, stress ratio

INTRODUCTION

Fiber-reinforced composites are widely used in aerospace, marine, automotive and advanced engineering applications in recent years, due to their high-quality mechanical properties. However, these structures always suffer cyclic fatigue loadings during service life, such as aircraft wings, helicopter blades, wind turbine blades and so on [1]. As a consequence, one important issue during the design of these composite structures is the fatigue damage assessment: the strength and durability of the composite structural components must take into account the typical damage

phenomena occurring under in-service loading. The fatigue behavior of fiber-reinforced composites is quite different from the one of metals [2], due to their anisotropy and heterogeneity characteristics, and the multi-scale nature of the damage processes and non-linear damage evolution during loading [3]. Therefore, it is important to understand the mechanisms associated to fatigue damage and to predict the long-term fatigue strength and life for fiber-reinforced composites under complex cyclic fatigue loading.

The fatigue damage failure process of fiber-reinforced composites involves a number of different failure mechanisms and interactive coupling effects. The different types of damage include fiber fracture, matrix cracking, matrix crazing, fiber buckling, fiber–matrix interface failure, delamination among composite plies and the effect of shear-induced diffuse damage on transverse cracks in fiber-reinforced composites, which has been already investigated through experimental [4] and theoretical methods [5], respectively. In addition, the fatigue performance of composites is also affected by the constituents of composite system, reinforcement structure, lay-up sequence, residual stress due to manufacturing process [6] and stress ratios [7-9] from external loading conditions. In order to simulate the fatigue damage behavior and to predict fatigue life of fiber-reinforced composites, in recent years several methodologies that implement progressive failure analysis and appropriate constitutive models with damage accumulation laws have been developed. In open literature, fatigue progressive damage models have been extensively established from macro to microscopic scales by means of theoretical analysis methods, finite element solutions and experiments [10-17]. Montesano et al [18] have established a damage mechanics based model that takes into account local multiaxial stresses as well as variable amplitude cyclic loading. The numerical results from that model showed the capability of that approach to predict the evolution of the damage and the degradation of the material properties in a triaxially braided carbon fiber polymer matrix component. Krüger and Rolfes [19] have presented a new layer-based fatigue damage model (FDM) for laminated multidirectional laminates in general states of plane stress. The stiffness and strength degradation were simulated using a Finite Element (FEM)

analysis, and the stress redistributions and sequence effects were also analyzed. Eliopoulos and Philippidis [20] developed an anisotropic non-linear constitutive model implementing progressive damage concepts to predict the residual strenght/stiffness and life of composite laminates subjected to multiaxial variable amplitude cyclic loading. In-plane mechanical properties of the material were fully characterized at the ply level while static or fatigue strength of any multidirectional stacking sequence can be predicted. Paepegem and Degrieck [21] established a phenomenological residual stiffness model to predict the stiffness degradation and possible permanent strains in fibre-reinforced polymers under in-plane fatigue loading. The stress-strain-damage relationships and the damage growth rate equations were developed and explained thoroughly. Montesano and Singh [22] have developed a multi-scale damage model combining synergistic damage mechanics with an energy-based damage evolution framework to predict the evolution of sub-critical matrix cracks in different plies under multiaxial loading, the ply crack density evolution and the laminate stiffness degradation. Quaresimin et al [23] investigated the very early stages of the damage evolution under a uniaxial cyclic tensile loading by testing [45/-45/0]s glass/epoxy specimens. In that work the first event observed for the damage initiation was multiple micro-cracks in the interfiber region of the 45 °ply, with a specific inclination with respect to the fibers. However, all the studies cited above mainly focus on the evaluation of the fatigue damage behavior, little attempt has been made to interpret the fatigue damage propagation and the effect of complicated loading mode such as stress ratio on fatigue damage growth, as well as the fatigue damage mechanisms for fiber-reinforced composites at meso-scale.

Continuum damage mechanics (CDM) is a mathematical and experimental description of the damage accumulation and growth due to changes of the material microstructure. On the basis of CDM theory, Pierre Ladevèze and his group established meso-scale damage models to describe the strength deterioration of composites under static loading. It is assumed that the behavior of any stratified structure can be described through two families of basic damageable constituents: the elementary layer and the interlaminar interface, and damage is considered uniform

through the thickness of individual layers of composites [24-27]. In these models two damage mechanisms are introduced. The first is related to the diffuse intralaminar damage associated with the fiber/matrix debonding in the ply and with small transverse cracks in the matrix. The second damage mechanism is associated with diffuse interlaminar damage linked to the formation of micro-voids in the matrix of the interlaminar interface, resulting in a reduced stiffness of the interlaminar interface with no visible delamination (Fig. 1 [27]). Therefore, the diffuse damage at the elementary ply scale can be modelled by a stiffness decline of the material along the axial, transverse and shear directions.

It is essential to extend the meso-scale damage model associated to static loading to complicated cyclic fatigue configuration. Also, it is quite important to investigate the fatigue damage behaviors and to develop new fatigue prediction methodologies for fiber-reinforced composites at meso-scale levels.
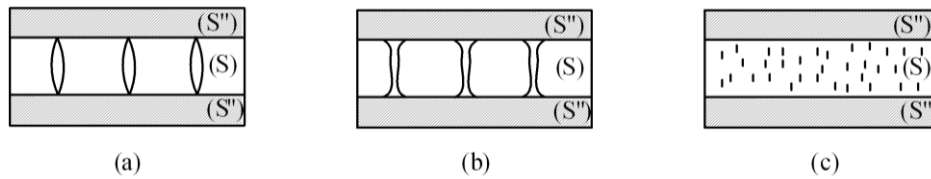

Fig. 1 Mechanisms of degradation on meso-scale: (a) transverse matrix microcracking; (b) local delamination; (c) diffuse damage [27]

In this paper we aim to establish a new fatigue damage meso-model in which the CDM theory is applied with the use of damage variables at the meso-scale of elementary plies and stress ratios to account for the complex fatigue loading history. The model is able to determine the fatigue damage growth at meso-scale and to predict the fatigue life of unidirectional composite laminates with arbitrary fiber orientation under different stress ratios. In this approach the progressive growth of diffuse damage is evaluated by establishing three groups of damage growth rate equations (along the axial, transverse and shear directions) according to continuum damage mechanics. We also introduce a non-dimensional effective stress [8, 9] to build a new fatigue diffuse damage meso-model that considers the effects of the fiber orientation and the stress ratios on the off-axis fatigue behavior of unidirectional

fiber-reinforced composite laminates. We then evaluate the validity of the proposed fatigue damage meso-model using data from the principal damage variables occurring in tension-tension cyclic loading under high-low stress levels and different stress ratios by GFRP and CFRP unidirectional composite laminates under different stress ratios with constant amplitude and frequency conditions [7, 8]. The results from the model are therefore discussed and show the viability of the proposed approach to predict on and off-axis fatigue damage propagation in composites.

FATIGUE DAMAGE MESO-MODEL

The present fatigue damage meso-scale model for unidirectional plies is developed within the framework of the thermodynamics in irreversible phenomena. Under the assumption of plane stresses and small perturbations, the strain energy of the ply can be written in the following form:

$$W_D = \frac{1}{2}\left[\frac{\langle\sigma_{11}\rangle_+^2}{E_{11}^0(1-D_{11})} + \frac{\langle\sigma_{11}\rangle_-^2}{E_{11}^0} - 2\frac{\upsilon_{12}^0}{E_{11}^0}\sigma_{11}\sigma_{22} + \frac{\langle\sigma_{22}\rangle_+^2}{E_{22}^0(1-D_{22})} + \frac{\langle\sigma_{22}\rangle_-^2}{E_{22}^0} + \frac{\tau_{12}^2}{G_{12}^0(1-D_{12})} \right] \tag{1}$$

Where E_{11}^0, E_{22}^0 and G_{12}^0 represents the initials stiffness of fiber, transverse and shear direction in plane, respectively. $\langle \ \rangle_+$ is defined as the positive part and $\langle \ \rangle_-$ as the negative parts. Consequently, when $\sigma_{22} \leq 0$, micro-cracks are closed and no noticeable damage occurs. Three damage indicators, which are constant through the thickness, pertain to the following mechanisms: Fiber breakage D_{11} (along the axial direction), matrix micro-cracking D_{22} (along the transverse direction) and deterioration of the fiber-matrix bonds D_{12} (along the shear direction).

From this potential, thermodynamic forces associated with the tension and shear internal variables D_{ij} $(i, j = 1, 2 \text{ and } i < j)$ are defined:

$$Y_{ij} = \frac{\partial W_D}{\partial D_{ij}} = \frac{\sigma_{ij}^2}{2E_{ij}^0\left(1-D_{ij}\right)^2} \tag{2}$$

The damage growth rates dD/dN correspond to the damage kinetics and are expressed as a function of the thermodynamic forces Y_{ij}, which are also connected to

the applied stress σ_{ij}. Therefore, a typical damage growth equation for a continuum fatigue damage variable D can be represented as:

$$\frac{dD_{ij}}{dN} = \mathbf{f}\left(D_{ij}, \sigma_{ij}, R, N, p\right) \tag{3}$$

Where $\mathbf{f}$ defines a fatigue damage function, the parameters σ_{ij}, R, N and p denote applied maximum stress, stress ratio, number of fatigue cycles and a history dependent parameter, respectively.

THE EFFECT OF STRESS RATIOS

Under realistic service conditions most structural components made from multidirectional composite laminates are subjected to complex fatigue loading histories characterized by changes in the amplitude, mean stress, frequency and waveform of the cyclic loading. As a significant influence factor the effect of the stress ratios on the off-axis fatigue behavior of unidirectional composites should not be therefore ignored. Therefore, it is necessary to develop appropriate fatigue damage models to study the fatigue damage accumulation at meso-scale and to predict the fatigue life of off-axial unidirectional composite laminates under different stress ratio conditions.

In order to incorporate the sensitivity to different loading modes, the stress ratio R, the alternating stress σ_a and mean stress σ_m have the relationships as

$R = \sigma_{\min} / \sigma_{\max}$, $\sigma_a = 1/2(1-R)\sigma_{\max}$ and $\sigma_m = 1/2(1+R)\sigma_{\max}$.

A non-dimensional scalar quantity Ψ [9] has been defined as:

$$\Psi = \frac{\sigma_a}{\sigma_B - \sigma_m} = \frac{(1-R)\sigma_{\max}}{2\sigma_B - (1+R)\sigma_{\max}} \tag{4}$$

Where σ_B is static failure strength. The modified fatigue strength ratio Ψ is a useful measure for the off-axis fatigue behavior of unidirectional composites and fatigue behavior of metals [28] at different stress ratios.

The non-dimensional effective stress [8, 9] for orthotropic materials based on the Tsai–Hill static quadratic interaction failure criterion has been defined as:

$$\sigma^* \equiv \sqrt{G_{ijkl}\sigma_{ij}\sigma_{kl}} = \sqrt{\left(\frac{\sigma_{11}}{X}\right)^2 - \frac{\sigma_{11}\sigma_{22}}{X^2} + \left(\frac{\sigma_{22}}{Y}\right)^2 + \left(\frac{\tau_{12}}{S}\right)^2} \tag{5}$$

Where X, Y and S represent the longitudinal, transverse and shear strength, respectively, in the case of plane stress. Similarly, the maximum non-dimensional effective stress can be uniquely decomposed as $\sigma^*_{max} = \sigma^*_a + \sigma^*_m$. The scalar quantities σ^*_a and σ^*_m represent the normalized alternating stress and normalized mean stress, respectively.

Considering the static failure condition $\sigma^*_{max} = \sigma^*_a + \sigma^*_m$ and the analogy with Eq. 4, the modified non-dimensional effective stress [9] is derived as follows:

$$\Sigma^* = \frac{\sigma^*_a}{1-\sigma^*_m} = \frac{(1-R)\sigma^*_{max}}{2-(1+R)\sigma^*_{max}} \tag{6}$$

When off-axis specimens are subjected to fatigue loading along the axial direction, the non-dimensional effective stress σ^*_{max} associated with the maximum fatigue stress σ_{max} can be expressed as:

$$\sigma^*_{max} = \sigma_{max}\sqrt{\frac{\cos^4\theta}{X^2} - \frac{\cos^2\theta\sin^2\theta}{X^2} + \frac{\sin^4\theta}{Y^2} + \frac{\sin^2\theta\cos^2\theta}{S^2}} \tag{7}$$

Therefore, the relationship between the maximum stress σ_{max} and the modified non-dimensional effective stress Σ^* is obtained as follows:

$$\sigma_{max} = \frac{2\Sigma^*}{\Omega(\theta)[(1-R)+(1+R)\Sigma^*]} \tag{8}$$

Where $\Omega(\theta) = \sqrt{\dfrac{\cos^4\theta}{X^2} - \dfrac{\cos^2\theta\sin^2\theta}{X^2} + \dfrac{\sin^4\theta}{Y^2} + \dfrac{\sin^2\theta\cos^2\theta}{S^2}}$ is orientation factor.

In this paper, the damage growth rate equation is prescribed following the form of the Kachanov-Rabotnov equation [29]:

$$\frac{dD_{ij}}{dN} = \frac{A_{ij}\left(\Sigma^*_{ij}\right)^{n_{ij}}}{\left(1-D_{ij}\right)^{B_{ij}}} \qquad (i,j=1, \text{and } i<j) \tag{9}$$

Where A_{ij}, n_{ij} and B_{ij} are material parameters associated to the axial, transverse and in-plane shear directions, respectively.

Replacing Eq. (2) and (8) into Eq. (9), the meso fatigue damage growth equations for three directions in-plane are derived as:

$$\frac{dD_{ij}}{dN} = \frac{A_{ij}}{\left(1-D_{ij}\right)^{B_{ij}}} \left(\frac{\sigma_{\max}\Omega(\theta)(1-R)}{2-\sigma_{\max}\Omega(\theta)(1+R)} \right)^{n_{ij}} \quad (i, j = 1, 2 \text{ and } i < j) \qquad (10)$$

According to Eq. (10), the effects of stress ratios on fatigue damage growths for fiber breakage, matrix cracking and fiber/matrix debonding in-plane and on the fatigue behaviors for off-axial unidirectional composites under different multiaxial cyclic loading modes are all taken into account.

APPLICATION TO OFF-AXIAL FATIGUE BEHAVIOR

Material parameter identification

The material parameters in these damage growth equations were determined by fitting to the typical $S-N$ relationships for three groups of fatigue experiment data under R=0 in Ref [7, 8], shown in Fig. 2 and Fig. 3, respectively. The solid lines in Fig. 2 and Fig. 3 indicate the master $S-N$ relationships identified for respective groups of the basic fatigue experiment data. The values of parameters involved by the master fatigue damage growth equations are listed in Table 1 and Table 2, for unidirectional glass/epoxy and carbon/epoxy laminates, respectively.
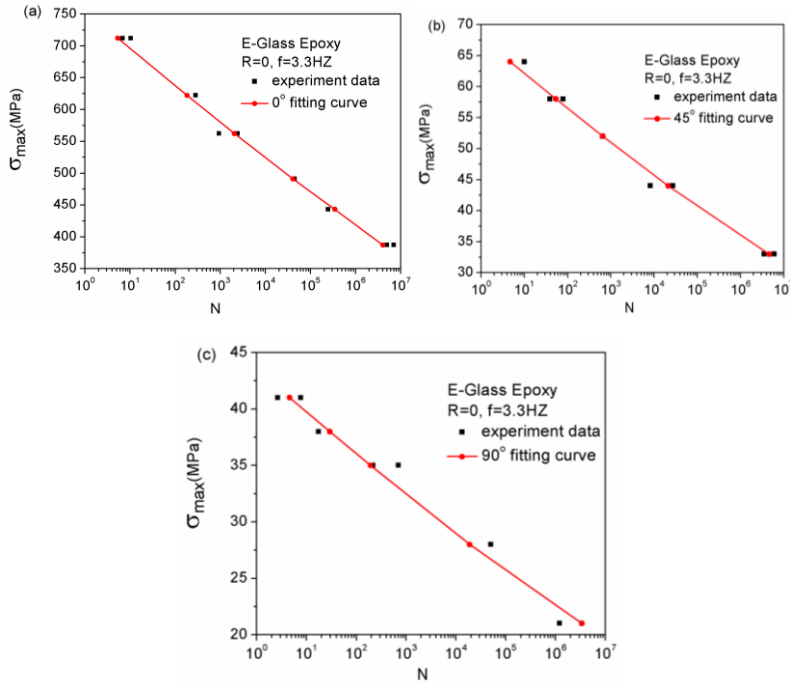

Fig. 2. Fitting *S-N* relationships for GFRP composite lamina under *R*=0: (a) 0°, (b) 45° (c) 90°

Table 1 Parameter determination for E-Glass Epoxy composites

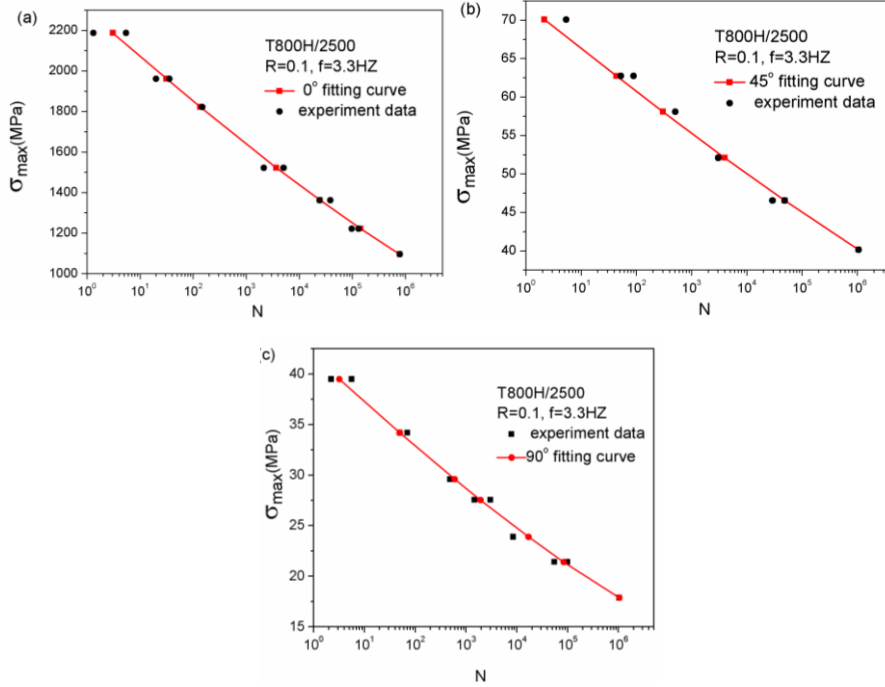| parameter	n_{ij}	A_{ij}	B_{ij}
0° ($i=j=1$)	14.0293	1.6745	1.3851
45° ($i=1, j=2$)	13.2293	2.0513	1.6536
90° ($i=j=2$)	12.6520	1.2315	1.1128

Fig. 3. Fitting S–N relationships for CFRP composite lamina under R=0 (a) 0° (b) 45° (c) 90°

Table 2 Parameter determination for Carbon/Epoxy composites

parameter	n_{ij}	A_{ij}	B_{ij}
0° ($i=j=1$)	11.6994	5.0451	1.1121
45° ($i=1, j=2$)	14.4612	4.1345	1.8725
90° ($i=j=2$)	10.6553	4.9106	0.7716

Failure Criterion

In this modelling, fatigue damage growths along axial, transverse and shear directions on the ply scale (fiber breakage, matrix micro-cracking and fiber/matrix debonding) are coexisting. Incorporating three sorts of damage, the fatigue failure criterion of fiber-reinforced unidirectional composite laminates is proposed as the determinant of coefficient of damaged stiffness matrix for the lamina is zero, which is equivalent to damage variable $D_{ij} = 1$ ($i, j = 1, 2$ and $i < j$).

Off-axis fatigue simulation

In order to obtain the quantificational fatigue behavior of off-axis unidirectional composite laminates, the process of fatigue damage growth on meso-scale is

simulated in the following procedure:

(a) In view of three damage modes in-plane, according to Eq. (10), two damage extremums for minimum status and maximum status are considered in the first calculation, respectively. It's assumed that the unidirectional composites have no initial damage, namely $D_{ij}^{initial} = 0$. Therefore, the initial damage increment either $\Delta D_{ij\,min}^{0}$ or $\Delta D_{ij\,max}^{0}$ could be determined by Eq. (10) and as a consequence, the corresponding initial cycle increment $\Delta N_{ij\,min}^{0}$ or $\Delta N_{ij\,max}^{0}$ could be obtained as well. Then, the initial cycle increment $\Delta N_{ij\,min}^{0}$ or $\Delta N_{ij\,max}^{0}$ is substituted into the other two damage evolution equations, respectively, in order to get the rest damage increments $\Delta D_{ij} = f_{ij}(\Delta N_{ij\,max/min}^{0})$ in other two different directions, where $i, j = 1, 2$ and $i < j$. So these three diffuse damage increments under the circumstance of either minimum or maximum extremums for first cyclic number are all obtained, respectively.

(b) Calculate the new damage fields for axial, transverse and shear directions after the first cyclic damage increment as follows:

$$D'_{ij} = D_{ij} + \Delta D_{ij} \qquad i, j = 1, 2 \quad \text{and} \quad i < j \qquad (11)$$

Where D'_{ij} refers to the new damage variables along axial, transverse and shear directions, respectively. Since the structural changes on meso-scale are characterized by a macroscopic stiffness reduction, the value of damage variable D is located between zero (initial material state) and one (final failure).

(c) Judge whether the new damage fields satisfy the failure criterion. If it is satisfied, the fatigue life of unidirectional composite laminates is $N = \sum \Delta N$; if not, the steps are repeated to step (a) until the failure criterion is satisfied.

   It must be emphasized that the value of damage increment ΔD_{ij} should be small enough to make sure a convergence result of N. The flow chart of this procedure is shown in Fig. 4.
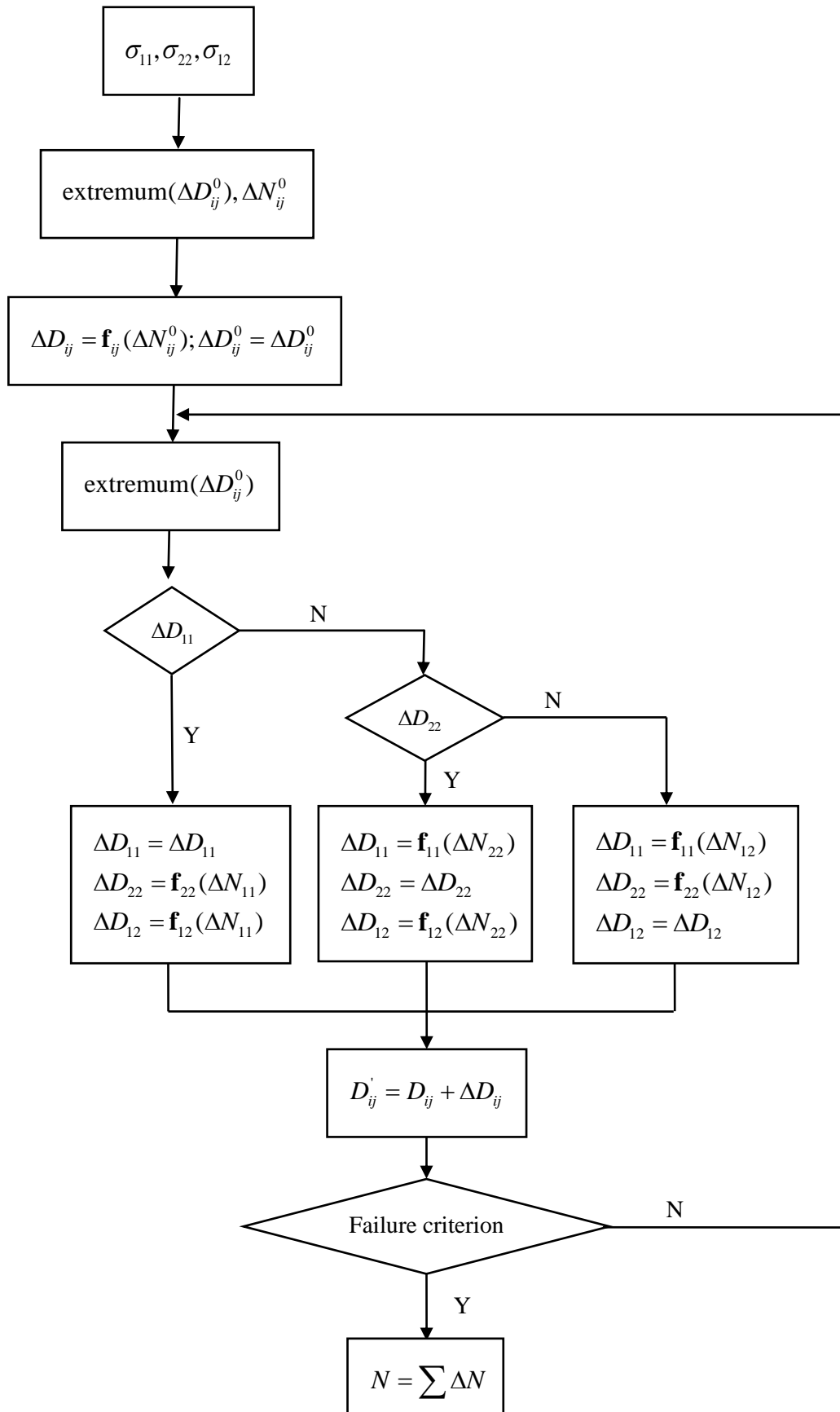
Fig. 4 Flow chart of the present numerical simulation

RESULTS AND DISCUSSION

The parameters in fatigue damage growth equations along axial, transverse and shear directions are determined by the fatigue tests of 0°, 90°, 45° GFRP and CFRP unidirectional composite laminates, respectively. Then the comparisons between the results of numerical prediction and experiment for 19° unidirectional glass/epoxy composite lamina under $R=0.5$ are reported in Table 3. Similar comparisons for 10°, 30° unidirectional carbon/epoxy composite laminas under $R=0.5$ are presented in Table 4 and Table 5 as well. In Table 3-Table 5, $\text{Log}N_{50,i}^{\exp}$ refers to the mean logarithmic fatigue life of the experiment, $\text{Log}N_i^{pred}$ refers to the logarithmic fatigue life of predicting model, subscript i refers to the stress level and $error_i$ is the relative error defined as

$$error_i = \left(\frac{\text{Log } N_i^{pred} - \text{Log } N_{50,i}^{\exp}}{\text{Log } N_{50,i}^{\exp}} \right)^2 \tag{12}$$

Table 3 Comparison between fatigue life prediction and experiment data for 19 °unidirectional GFRP lamina under R=0.5

i	$\sigma_{\max}$	$\text{Log}N_{50,i}^{\exp}$	$\text{Log } N_i^{pred}$	$error_i$
1	145	2.4004	2.5775	5.44 e-03
2	135	3.5467	3.6123	3.42e-04
3	126	4.3650	4.5729	2.27 e-03
4	113	5.7253	5.8848	7.76e-04

Table 4 Comparison for 10 °unidirectional CFRP lamina between fatigue life prediction and experiment data under R=0.5

i	$\sigma_{\max}$	$\text{Log}N_{50,i}^{\exp}$	$\text{Log } N_i^{pred}$	$error_i$
1	307	1.5419	1.5563	8.73 e-05
2	278	2.9363	2.9138	5.87e-05
3	252	4.1245	4.0540	3.06 e-04

Table 5 Comparison for 30 °unidirectional CFRP lamina between fatigue life prediction and experiment data under R=0.5

i	σ_{max}	$\text{Log}N_{50,i}^{exp}$	$\text{Log }N_i^{pred}$	$error_i$
1	106	1.9297	1.9590	2.31e-04
2	96	2.8527	2.8470	4.0e-06
3	81	4.2541	4.3578	5.95e-04

The predicting S–N relationships of 19°, 71° GFRP unidirectional composite laminates and 10°, 15°, 30° CFRP unidirectional composite laminates under different stress ratios are given in Fig. 5 and Fig.6, respectively. Fig. 5 exhibits that the fatigue life and residual strength of off-axis GFRP unidirectional composite laminates decreases when the fiber orientation increases under the same stress ratio, the similar tendency is shown in Fig. 6 as well. The results indicate that the predictions of fatigue life are in good agreement with experiment data of Ref [7, 8], the off-axis fatigue behavior of two types of unidirectional composites and its stress ratio R-dependence have favorably been described by the fatigue damage meso-model.
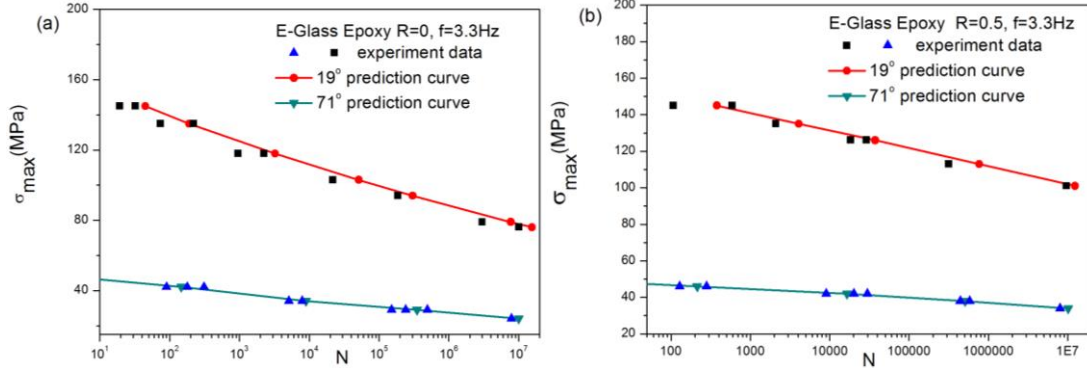

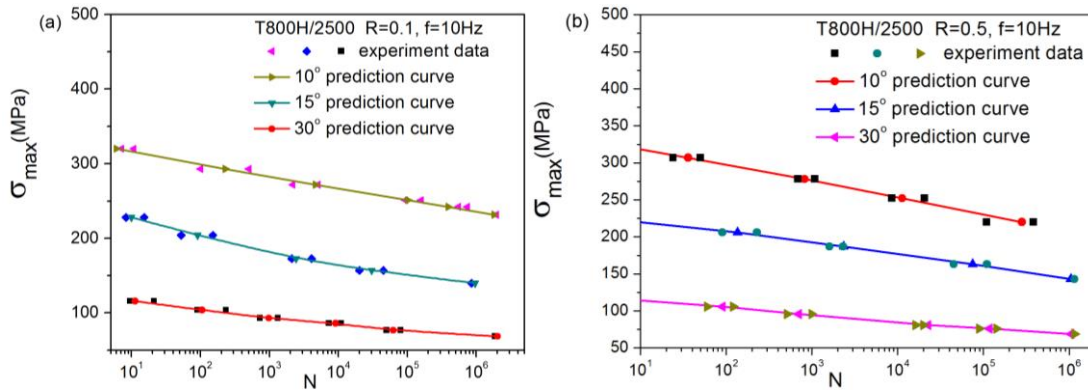Fig. 5. 19° and 71° GFRP unidirectional laminate predicting S–N relationships (a) under R=0 (b) under R=0.5

Fig. 6. 10°, 15° and 30° CFRP lamina predicting S–N relationships under (a) R=0.1 and (b) R=0.5

The off-axial fatigue behaviors of 19° unidirectional composite laminate under stress ratios $R=0$ and $R=0.5$ are compared in Fig. 7 (a); furthermore, the predicting *S-N* curve group under different stress ratios $R=0, 0.3, 0.5, 0.8$ is shown in Fig.7 (b) as well. For a given maximum stress in the tension-tension cyclic loading, the off-axis fatigue life of the unidirectional composite laminate increases with the increasing stress ratio *R*. This behavior is consistent with the one observed in open literature for continuous and short fiber reinforced composites predicted by different methodologies [8, 11, 30, 31]. The interpretation for this trend is that increasing the stress ratio *R*, reduces the stress amplitude σ_{amp} (for a constant maximum stress, $\sigma_{amp} = \sigma_{max}(1-R)/2$) of the load regime, leads to a flatter *S-N* curve as well as a slower fatigue degradation and damage accumulation rates. At higher stress ratios, the material is being subjected to lower stress amplitudes, and hence it will have to endure lower stress/strain gradients in the fiber, matrix and at the fiber/matrix interface. It would in turn lead to a reduced crack growth rates and less significant fatigue strength degradation with increasing number of cycles [32-34].
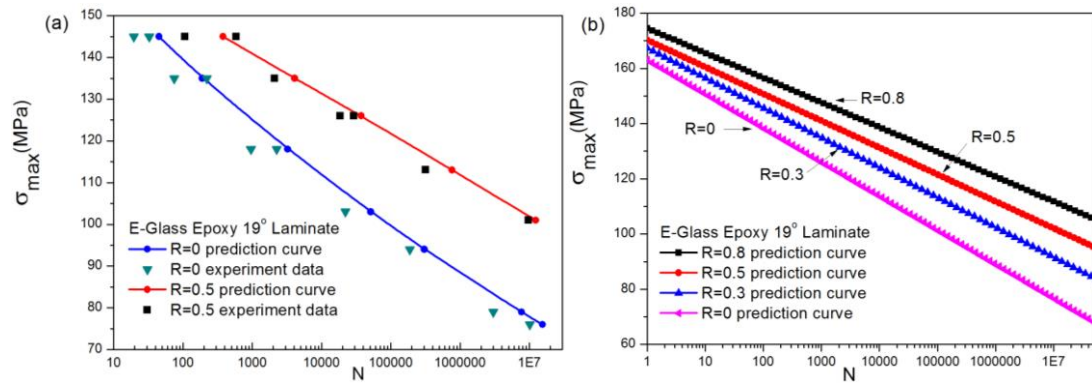

Fig. 7. Off-axis fatigue behavior for the E-Glass Epoxy 19° unidirectional composites: (a) comparison of the fatigue life between $R=0$ and $R=0.5$ (b) prediction *S-N* curves group at $R=0, 0.3, 0.5, 0.8$

The fatigue meso-damage growth for the 19° GFRP unidirectional composite laminate under high and low stress levels is shown in Fig.8. The figure shows that the relationship between the transverse damage D_{22} (a), shear damage D_{12} (b), axial damage D_{11} (c) and cyclic number *N* are almost the same during the whole entire fatigue damage growth progress of the composite materials. One can observe a rapid

damage accumulation during the first cycles, then a slow and steady damage growth followed by a sudden failure on the last stage.
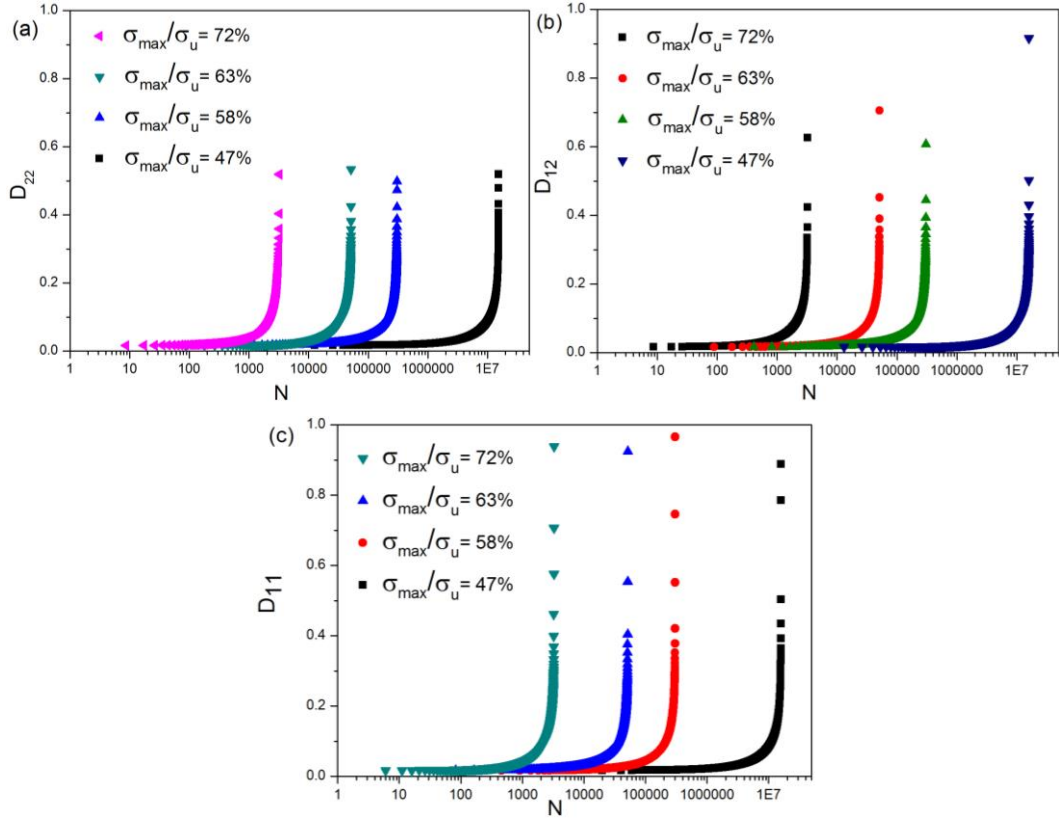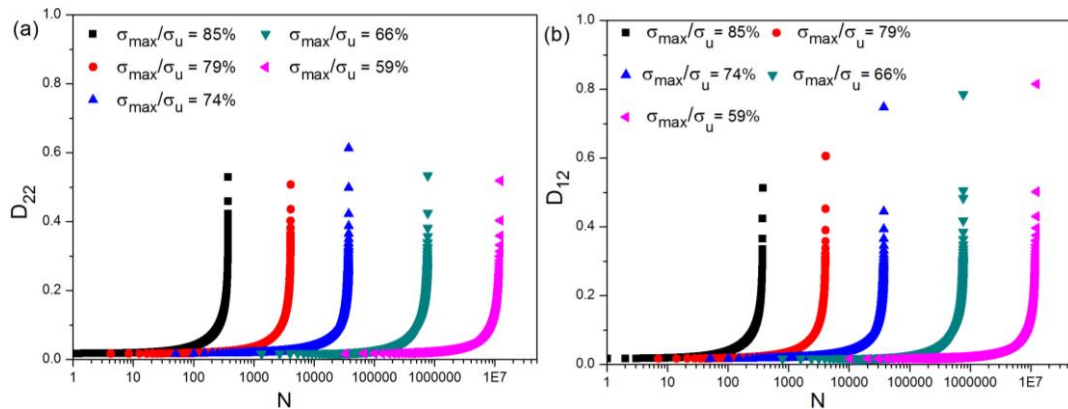

Fig. 8. Fatigue damage growths on meso-scale for GFRP 19° unidirectional composite laminate under R=0: (a) transverse damage D_{22}, (b) shear damage D_{12}, (c) axial damage D_{11}

The elastic modulus of the matrix is significantly smaller than the one of the fiber and the interface in meso-constituents [24]. The transverse damage D_{22} (i.e., matrix microcracking) is lower than 0.6 for the whole stress levels (Fig.8 (a)). This feature demonstrates that the transverse matrix microcracks always occur during the early stages of the damage growth, and then increase and expand until the cracks in each ply reach to equilibrium or saturation, a stage which is denominated the characteristic damage state (CDS) [35]. The fatigue damage growth of the shear damage D_{12} is however different under high and low stress levels (Fig.8 (b)). At high stress levels ($\sigma_{max}/\sigma_u = 72\%$) D_{12} is within the range of 0.65-0.75, however, at low stress levels ($\sigma_{max}/\sigma_u = 47\%$) D_{12} now approaches the unity value, which means that the shear damage D_{12} (fiber/matrix interfacial debonding) plays a part at low cyclic loading and provides an effect to the final failure of the composite materials. This

15

phenomenon can be interpreted by considering that during the second stage of the fatigue damage growth transverse microcracks extend through the thickness of the off-axis plies. Interfacial debonding microcracks perpendicular to transverse cracks then occur, which are caused by the tensile stress along the crack axis ahead of the primary transverse microcracks [35]. In Fig.8 (c) the axial damage D_{11} almost reaches the value of 1 on both high and low stress levels, which means that the fiber breakage generates a significant effect on the damage growth progress and dominates the final failure of the 19° GFRP unidirectional composite laminate. This feature is interpreted by considering that scattered fiber failures begin to initiate locally during the early stage of the damage growth, followed by fiber breakage growths with cyclic loading until the neighboring zones of fiber failures are joined together, and the specimen is weakened with an eventual catastrophic failure [35]. It should be also emphasized that these fatigue damage mechanisms are interactive and coupled together. No individual damage mechanism single handedly dominates a distinct phase of the total life of a component; these mechanisms occur more or less simultaneously.

The fatigue damage growths of D_{22}, D_{12} and D_{11} (in transverse, shear and axial directions) for 19° GFRP unidirectional composite laminates under R=0.5 are discussed as well and shown in Fig.9, respectively, which have the similar tendency of damage growth under R=0. It is shown that axial damage D_{11} and shear damage D_{12} both increase with the increasing of cyclic number N and contribute to the final failure under low stress level the same as scenario R=0. However, the transverse fatigue damage D_{22} is almost invariable in the whole damage growth stage.
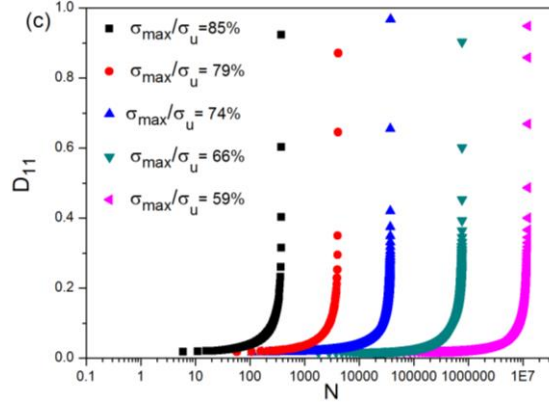
Fig. 9. Fatigue damage growths on meso-scale for GFRP 19° unidirectional composite laminate under R=0.5: (a) transverse damage D_{22}, (b) shear damage D_{12}, (c) axial damage D_{11}

For most cases, the fatigue tests under different stress ratios for the same stress levels are not usually carried out, therefore, the paper doesn't compare the fatigue damage D_{22}, D_{12} or D_{11} between R=0 and R=0.5 with the same stress level. The proposed fatigue damage meso-model is also applicable to tension-tension (T-T) cyclic loading, in particular for the scenarios describing tension-compression (T-C) and compression-compression (C-C) cyclic loading. The formulation of Eq. (10) and the failure criterion should be however modified to consider the compressive component of the fatigue damage [36].

CONCLUSIONS

A new fatigue damage meso-model considering the stress ratio effect as well as the fiber-orientation effect on the off-axis fatigue behavior of unidirectional composites was developed. The non-dimensional effective stress that accounts for the effect of stress ratio was introduced and three groups of diffuse damage growth equations on elementary ply scale were established based on continuum damage mechanics theory. Three fatigue damage growths of axial, transverse and shear directions under different stress ratios were studied, respectively. Fatigue life of off-axis unidirectional composite laminates with arbitrary fiber orientation under different stress ratios were predicted by numerical simulation and compared with the experimental data as well. The results demonstrated that the proposed fatigue damage meso-model can adequately describe the off-axis fatigue damage behaviors and predict off-axis fatigue life of glass/epoxy and carbon/epoxy unidirectional composite

laminates with arbitrary fiber orientation under constant amplitude tension-tension cyclic loading over a range of stress ratios.

Acknowledgments

References

[1] R.Brighenti, A. Carpinteri, D. Scorza, Micromechanical crack growth-based fatigue damage in fibrous composites, Int. J. Fatigue 82 (2016) 98-109.

[2] D.Y. Zhang, J. Hong, Y.H. Ma, L.L. Chen, A probability method for prediction on High Cycle Fatigue of blades caused by aerodynamic loads, Adv. Eng. Softw. 42 (2011) 1059-1073.

[3] D. Vasiukov, S. Panier, A. Hachemi, Direct method for life prediction of fibre reinforced polymer composites based on kinematic of damage potential, Int. J. Fatigue 70 (2015) 289-296.

[4] H. Nouri, G. Lubineau, D. Traudes, An experimental investigation of the effect of shear-induced diffuse damage on transverse cracking in carbon-fiber reinforced laminates, Compos. Struct. 106 (2013) 529-536.

[5] W.J. Zhang, Z.G. Zhou, P. Zheng, S.Y. Zhao, The fatigue damage mesomodel for fiber-reinforced polymer composite lamina. J. Reinf. Plast. Comp. 33 (2014) 1783-1793.

[6] G. Lubineau, Estimation of residual stresses in laminated composites using field measurements on a cracked sample, Compos. Sci. Technol. 68 (2008) 2761-2769.

[7] H.E. Kadi, F. Ellyin, Effect of stress ratio on the fatigue of unidirectional glass fibre/epoxy composite laminae, Compos. 25 (10) (1994) 917-924.

[8] M. Kawai, A Phenomenological Model for Off-axis Fatigue Behavior of Unidirectional Polymer Matrix Composites under Different Stress Ratios, Compos. Part A 35 (7-8) (2004) 955-963.

[9] M. Kawai, K. Kato, Effects of R-ratio on the off-axis fatigue behavior of unidirectional hybrid GFRP/Al laminates at room temperature, Int. J. Fatigue 28 (2006) 1226-1238.

[10] S. Shiri, M. Yazdani, M. Pourgol-Mohammad, A fatigue damage accumulation model based on stiffness degradation of composite materials, Mater. Des. 88 (2015) 1290-1295.

[11] W.J. Zhang, Z.G. Zhou, B.M. Zhang, S.Y. Zhao, A phenomenological fatigue life prediction model of glass fiber reinforced polymer composites, Mater. Des. 66 (2015) 77-81.

[12] L. Toubal, M. Karama, B. Lorrain, Damage evolution and infrared thermography in woven composite laminates under fatigue loading, Int. J. Fatigue 28 (12) (2006) 1867-1872.

[13] H.J. Shen, W.X. Yao, Synergistic Damage Mechanic Model for Stiffness Properties of Early Fatigue Damage in Composite Laminates, P. Eng. 74 (2014) 199-209.

[14] F.Q. Wu, W.X. Yao, A Fatigue Damage Model of Composite Materials, Int. J. Fatigue 32 (1) (2010) 134-138.

[15] J.A. Mohandesi, B.Majidi, Fatigue Damage Accumulation in Carbon/epoxy Laminated Composites, Mater. Des. 30 (6) (2009) 1950-1956.

[16] J. Brunbauer, C. Gaier, G. Pinter, Computational fatigue life prediction of continuously fibre reinforced multiaxial composites, Compos. Part B 80 (2015) 269-277.

[17] D. Flore, K. Wegener, Modelling the mean stress effect on fatigue life of fibre reinforced plastics, Int. J. Fatigue 82 (2016) 689-699.

[18] J. Montesano, M. Selezneva, M. Levesque, Z. Fawaz, Modeling fatigue damage evolution in polymer matrix composite structures and validation using in-situ digital image correlation, Compos. Struct. 125 (2015) 354-361.

[19] H. Krüger, R. Rolfes, A physically based fatigue damage model for fibre-reinforced plastics under plane loading, Int. J. Fatigue 70 (2015) 241-251.

[20] E.N. Eliopoulos, T.P. Philippidis, A Progressive Damage Simulation Algorithm for GFRP Composites under Cyclic Loading. Part I: Material Constitutive Model, Compos. Sci. Technol. 71(5) (2011) 742-749.

[21] W.V. Paepegem, J. Degrieck, Modelling damage and permanent strain in fibre-reinforced composites under in-plane fatigue loading, Compos. Sci. Technol. 63 (5) (2003) 677-694.

[22] J. Montesano, C. V. Singh, Critical stiffness damage envelopes for multidirectional laminated structures under multiaxial loading conditions, Mater. Des. 91 (2016) 218-229.

[23] M. Quaresimin, P.A. Carraro, L. Maragoni, Early stage damage in off-axis plies under fatigue loading, Compos. Sci. Techno. 128 (2016) 147-154.

[24] G. Lubineau, P. Ladevèze, Construction of a micromechanics-based intralaminar mesomodel, and illustrations in ABAQUS/Standard, Comp. Mater. Sci. 43 (2008) 137-145.

[25] F. Daghia, P. Ladevèze, A Micro–meso Computational Strategy for the Prediction of the Damage and Failure of Laminates, Compos. Struct. 94 (12) (2012) 3644-4653.

[26] E. Obert, P. Ladevèze, Micro and Meso Modeling of Woven Composites: Transverse Cracking Kinetics and Homogenization, Compos. Struct. 117 (2014) 212-221.

[27] G. Lubineau, P. Ladevèze, D. Violeau, Durability of CFRP laminates under thermomechanical loading: A micro–meso damage model, Compos. Sci. Technol. 66 (2006) 983-992.

[28] R.W. Landgraf, The resistance of metals to cyclic deformation. Achievement of high fatigue resistance in metals and alloys, ASTM STP 467 (1970) 3-36.

[29] Y. N. Rabotnov, Creep Problems of Structural Members, 1969, North-Holland.

[30] M. Kawai, K. Yano, Probabilistic anisomorphic constant fatigue life diagram approach for prediction of P-S-N curves for woven carbon/epoxy laminates at any stress ratio, Compos. Part A 80 (2016) 244-258.

[31] P.K. Mallick, Y.X. Zhou, Effect of mean stress on the stress-controlled fatigue of a short E-glass fiber reinforced polyamide-6,6, Int. J. Fatigue 26 (2004) 941-946.

[32] D.D. Samborsky. Fatigue of E-glass fiber reinforced composite materials and substructures. MSc, 1999. Montana State University: Bozeman.

[33] J.F. Mandell, D.D. Samborsky, P. Agastra. Composite materials fatigue issues in wind turbine blade construction, in SAMPE 2008. 2008. Long Beach.

[34] D.D. Samborsky, T.J. Wilson, J.F. Mandell. Comparison of tensile fatigue resistance and constant life diagrams for several potential wind turbine blade laminates, 2006. American Institute of Aeronautics and Astronautics: Reston.

[35] R. Talreja, Damage and fatigue in composites-A personal account, Compos. Sci. Technol. 68 (2008) 2585-2591.

[36] W.V. Paepegem, J. Degrieck, A new coupled approach of residual stiffness and strength for fatigue of fibre-reinforced composites, Int. J. Fatigue 24 (7) (2002) 747-762.